Australian Earthquake Engineering Society 2014 Conference, Nov 21-23, Lorne, Vic

Earthquake forecasting - a review and combination logic to multilayer earthquake forecasting

Andreas Schäfer[1,2] & James Daniell[1,3] & Friedemann Wenzel[1]
[1] Geophysical Institute & Center for Disaster Management and Risk Reduction Technology (CEDIM), Karlsruhe Institute of Technology (KIT), Hertzstrasse 16, 76187, Karlsruhe, Germany.
[2] Ludwig-Maximilians-Universität München, Theresienstraße 41, 80333 Munich, Germany
[3] General Sir John Monash Scholar, The General Sir John Monash Foundation, Level 5, 30 Collins Street, Melbourne, Victoria, Australia 3000.

E-Mail: aschaefer.engineering@gmail.com

ABSTRACT:

For decades, earthquake prediction and forecasting has remained one of the most challenging tasks in modern geosciences. During this period, a great number of different algorithms have been developed to calculate earthquake forecasts from rather simple statistical methods for smooth seismicity to complex triggering algorithms incorporating Coulomb stress changes or seismic gap identification.

More than 20 methods have been reviewed and evaluated to identify the state-of-the-art in earthquake forecasting and to develop a clear catalogue of forecasting methods. In general, a sophisticated forecast is hard to achieve and applying just one of the methods may not lead to reliable results. Nevertheless, a detailed catalogue of these techniques provides a state-of-the-art in forecasting

A combined model out of different established forecasting algorithms, incorporating time-independent and time-dependent theories, is assembled to merge their advantages. Using retrospective forecasting tests, a scorecard weighting system of forecasting reliability is introduced for the weighting of a logic tree approach which can then be used for future applications in earthquake forecasting procedures globally.

Keywords: Earthquake forecasting, time-dependent, logic combination, method review catalogue

1. Introduction

Over the last two to three decades various pattern recognition algorithms have been developed to identify and track precursory phenomena for the prediction of earthquakes. One of the first methods proposed was the famous M8 algorithm of Kossobokov, [1986]. It was subsequently developed and advanced and is still in use today [Kossobokov, 2014]. Originally addressing the given magnitude >M8 earthquakes, additional versions for smaller magnitudes (M6.5 and M7.5 respectively) have been established. Other well-known methods such as the Reverse-Tracing of Precursors method of Shebalin [2006] have already gained media attention even after showing that the initial enthusiasm about predicted earthquakes was not maintained due to less successful results. While the methods mentioned above can be considered to be alarm-based, the alterations of RTL and RTM methods [Nagao, 2011; Huang, 2006] and the so-called Pattern Informatics approach [Holliday et al., 2005; Kawamura, 2014] investigate more long-term and large-scale deviations from the average earthquake activity indicating locations of either quiescence or increased activity.

Taking these methods on their own, each is limited to its assigned precursory track and each examines the occurrence of earthquakes with its own algorithm. Since most of the investigated precursor phenomena are still under debate [Kagan, 1997], because some of them only occur at certain locations while tracking only a specific type of precursory signal, some strong earthquake events have no precursor at all. A typical example of an unpredictable earthquake is the Christchurch sequence which happened without any precursor signal, or at least none that can currently be tracked. It is assumed that a multilayer approach, which is a superposition of multiple of the above mentioned methods, will lead to a significant increase in the predictive and forecasting capabilities.

Here, such a multilayer method is introduced, adopting multiple pattern search algorithms into one framework. Section 2 introduces the catalogue which has been assembled to identify possible candidate methods for subsequent analysis. Section 3 examines these methods in more detail and the respective modifications which have been implemented. Section 4 describes the assemblage of these methods and how they are combined into one earthquake forecast. Section 5 presents the results of a case study based on Californian earthquake data which are finally analyzed in Section 6.

2. Method Catalogue

A detailed earthquake forecasting method catalogue has been proposed by Schaefer et al. [2014] to review and analyze the state-of-the-art in earthquake forecasting methods and algorithms. Figure 1 shows the overview of all these different methods which are currently part of the catalogue (August 2014). While time-independent methods are all relatively similar in terms of their algorithms and the way they calculate earthquake forecasts, the largest diversity can be seen in the time-dependent approaches, where, for example, pattern search algorithms or epidemic methods are very popular. The catalogue does not evaluate the predictive and forecasting capabilities of each method, but rather catches the characteristics of each method and assembles short summaries for each within a single document.

To assemble a multilayer forecasting approach, it is important that each of the implemented methods provides a similar kind of forecast, addresses the same kind of target event (strong mainshocks or aftershocks), provides numerical stability and is not resource-intense in terms of computational time. Out of this consideration, three methods have been chosen to be combined into a single earthquake forecasting framework. Firstly, the Pattern Informatics (PI) method to identify long-term changes in seismicity; secondly, the RTM/RTL method to track

seismic quiescence before earthquakes; and finally, the Reverse-Tracing-of-Precursors (RTP) method. The RTP method introduces multiple pattern recognition functions, which are applied on earthquake chains, which are accumulations of earthquakes within space-time-boundaries. The M8 method was not selected since there is currently no free available publication which explains the algorithm in such a detail that it can be reproduced and implemented in this study.

	Method (Publication)	Description
Time-independent	Relative Intensity (Nanjo, 2010)	Smooth seismicity
	Asperity-based Likelihood Method (Gulia et al., 2010)	Smooth seismicity, local b-value
	HAZGRIDX (Akinci, 2010)	Smooth seismicity
	Adaptively Smoothed Seismicity (Werner et al., 2010)	Smooth seismicity, Dynamic kernel
	PEGASOS-EG1b (Burkhard & Grünthal, 2009)	Seismic Zonation
	Simple Smoothed Seismicity (Zechar & Jordan, 2010)	Smooth seismicity
Time-dependent	Pattern Informatics (PI) (Holiday et al., 2010)	Pattern Search
	Reverse-Tracing of Precursors (Shebalin et al., 2006)	Pattern Search, Alarm-based
	Epidemic-Type of Aftershock Sequences (ETAS) (Zhuang, 2010)	Epidemic, Aftershocks
	Doube-branching ETAS (Lombardi & Marzocchi, 2010)	Epidemic, Aftershocks, long vs. short-term
	Every Earthquake a Precursor According to Scale (Rhoades, 2007)	Epidemic, Precursor, Aftershocks
	Epidemic-Rate-Strain (Console et al., 2007)	Epidemic, Rate & State Friction
	Short-term Aftershock Probabilities (Gerstenberg et al., 2004)	Aftershock, Alarm-based
	Early Aftershock Statistics (Shebalin et al., 2011)	Pattern Search
	M8-Algorithm (Romachkova et al., 1998)	Pattern Search, Alarm-based
	Artificial Neural Networks (Reyes et al., 2013)	Machine-Learning, Alarm-based
	RTL/RTM-Method (Huang, 2006)	Pattern Search
Hybrid	Fault Slip and Smoothed Seismicity (Hiemer et al., 2013)	Smooth Seismicity, Focal Mechanisms
	Hybrid Seismicity Method (Chan et al., 2010)	Smooth Seismicity, Coulomb Stress Changes
	Long-term Stress Transfer (Falcone et al., 2010)	Coulomb Stress Changes, Interevent-time
	Seismic Hazard Inferred from Tectonics (Bird & Liu, 2007)	Kinematic Modelling, Fault Model
	Fault-oriented Earthquake Forecast (van Aalsburg et al., 2010)	Virtual Fault Model, Rate & State Friction

Figure 1: Overview of the earthquake methods and algorithms, which are part of the catalogue of Schaefer et al. [2014]. The methods denoted by a rectangle are chosen for further investigation for a multilayer forecasting framework.

3. Methods and Modifications

For the first prototype of a multilayer forecasting framework, three methods have been chosen to be adopted for this project. All three of these methods have been modified to fit into the multilayer framework and in terms of forecasting capabilities. Most of the modifications are related to adapt to the identification of precursory signals or in terms of computation speed. The most significant changes have been made to the Reverse-Tracing of Precursors (RTP) method, while the Pattern Informatics (PI) remained essentially unchanged. The combination of the methods to assemble them into a single layer-based method will be described in Chapter 3.

3.1 Reverse-Tracing of Precursors

The RTP method of Shebalin et al. [2006] is an alarm-based pattern recognition method which tracks so-called earthquake chains. These chains are estimated by analyzing the space time neighbourhood of each new occurring earthquake and, if other events do exist in the close vicinity of r_0 for space and t_0 for time, the events are connected to a chain. In case, the size of a chain exceeds a certain threshold value k, multiple pattern recognition functions are applied to analyze the occurrence pattern of the chain to identify possible precursory signals. In the original method, 8 functions have been used, whilst for the modification in this study only three have been implemented without modification, neglecting the other 5, but adding 2 additional functions, resulting in a total of 5 different functions. The 5 neglected functions have been tested and afterwards removed or replaced with new functions, since the originals e were either too time consuming for numerical calculation or insensitive for tracking precursory signals. A chain with n elements is evaluated in terms of precursory signal, providing that the youngest element of the chain is not older than 1 year and $n \geq 15$. The following 5 functions are then applied. The functions "*Activity*" f_1, "*Sigma*" f_2, and "*Speed*" f_3 analyze if a rise of activity is observable within the chain. The function "*Gamma*" f_4 searches for an increase in the magnitude correlation and f_5 "*Swarm*" identifies earthquake cluster processes. f_1, f_2 and f_4 are the three original functions from Shebalin et al. [2006].

Activity

$$f_1(t) = \frac{n}{t - t_1} \tag{2.1}$$

Sigma

$$f_2(t) = \sum_{i=1}^{n} 10^{M_i - M_{min}} \tag{2.2}$$

Speed

$$f_3(t) = \frac{n_{t<t_0}}{t_0} \tag{2.3}$$

Gamma

$$f_4(t) = \frac{1}{n_{M_i \geq \widetilde{M}}} \sum_{M_i \geq \widetilde{M}} (M_i - M_{min}) \tag{2.4}$$

Swarm

$$f_5(t) = \frac{1}{n} \sum_{i=1}^{n} \frac{\Delta r_i}{\tilde{r}} \tag{2.5}$$

With t_1 as the time of the oldest event in the chain, M_{min} is the minimum magnitude of the complete data and $n_{t<t_0}$ is the number of earthquakes which are not older than t_0. $n_{M_i \geq \widetilde{M}}$ is the number of earthquakes with a magnitude greater than $\widetilde{M}$ which is the median magnitude of the chain. Δr_i is the Euclidean distance between the chains centroid and the element i and $\tilde{r}$ is the respective median of these distances. Each of these functions is afterwards normalized by

$$\langle f_k \rangle(t) = \frac{f_k(t) - \overline{f_k(t)}}{\sigma_{f_k}} \tag{2.6}$$

where $\overline{f_k(t)}$ is the mean value of f_k and σ_{f_k} is the standard deviation of f_k up to time t, where k is from the function set $[f_1, \ldots, f_5]$. The different function results are combined as a simple product.

$$P(t) = \prod_{k=1}^{5} \langle f_k \rangle(t) \tag{2.7}$$

The predictive value $P(t)$ is then again normalized by removing the linear trend $P_{tr}(t)$ and dividing by its temporal standard deviation σ_P.

$$RTP(t) = \frac{P(t) - P_{tr}(t)}{\sigma_P} \tag{2.8}$$

To convert the RTP result into a map, the event locations of each earthquake chain have been assigned with their chain's respective pattern result $RTP(t)$ and then smoothed using a Gaussian kernel. Multiple chains can be active at the same time; thus, the predictive RTP layer at time t is a superposition of all smoothed pattern results, of which the youngest chain element is not older than 1 year.

3.2 RTL/RTM Method

The RTL/RTM Methods refer to the work of Nagao [2011] and Huang [2006], where various functions track spatio-temporal characteristics. For this study, two functions from Huang [2006] and one function from Nagao [2011] are combined, tracking temporal, spatial and magnitude correlations. The functions provide dimensionless factors, which approximately represent the standard deviation of the occurrence parameter.

$$R(x, y, t) = \left[\sum_{i=1}^{n} \exp\left(-\frac{r_i}{r_0}\right)\right] - R_{tr}(x, y, t) \tag{2.9}$$

$$T(x, y, t) = \left[\sum_{i=1}^{n} \exp\left(-\frac{t_i - t}{t_0}\right)\right] - T_{tr}(x, y, t) \tag{2.10}$$

$$M(x, y, t) = \left[\sum_{i=1}^{n} \mathrm{M_i}\right] - M_{tr}(x, y, t) \tag{2.11}$$

Where r_i is the distance between the position and event i, r_0 is the characteristic distance. Similarly, $t_i - t$ is the time since event i and t_0 the characteristic time period. $R_{tr}(x, y, t)$, $T_{tr}(x, y, t)$ and $M_{tr}(x, y, t)$ are the linear trends respectively. For the evaluation at a certain position and time, all events that are within $2r_0$ from the position and not older than $2t_0$ are taken into account.

$$RTM(x, y, t) = R(x, y, t) * T(x, y, t) * M(x, y, t) \tag{2.12}$$

As seen in Equation (2.12), the final RTM value is the product of the proposed tracking functions.

3.3 Pattern Informatics

The implementation of the pattern informatics is similar to that proposed by Holiday [2005] or Kawamura [2014]; thus the PI method will be briefly explained with all modifications outlined. The PI method divides the earthquake data into two equal periods $[t_0, t_1]$ and $[t_1, t_2]$ and compares the changes in seismicity. The length of these periods can be varied, and often chosen to be between 1 to 10 years. The activity is thus calculated and normalized in space and time for shorter varying time steps $[t_b, t_1]$ and $[t_b, t_2]$, where $t_0 \leq t_b \leq t_1$. For each time interval, the intensity, which represents the number of earthquakes at a certain location (or within a certain distance) over time, is calculated. Afterwards, the intensity change between the periods is calculated and normalized in space and time. This procedure is performed for multiple values of t_b, e.g. each with a difference of 30 days, ending up with multiple intensity values with $\Delta I_i(t_b, t_1 t_2)$ for each location i. The earthquake occurrence probability for a certain position i is then the absolute mean over time.

$$P_i(t_1 t_2) = \left|\overline{\Delta I_i(t_b, t_1 t_2)}\right| \tag{2.13}$$

$$\Delta P_i(t_1 t_2) = P_i(t_1 t_2) - \overline{P_i(t_1 t_2)} \tag{2.14}$$

The final PI map is afterwards normalized by dividing all values by their respective maximum value.

4. Multilayer Framework

The so-called multilayer framework combines the forecasting maps of various earthquake forecasting algorithms. This combination procedure assembles the advantages, but in the same way also the disadvantages of the respective methods. In this study, the three methods, introduced and modified in Chapter 3, are combined to take advantage of their distinct precursory identification patterns. All 3 methods use different ways to track precursory signals. In general, these precursory signals either do not occur for each earthquake event with an equal strength or might not occur at all and hence it has become important to track multiple patterns of precursory signals to reduce the probability of missing a certain event.
Since the multilayer framework is new, and most of the proposed sub-methods are based on alarm-based algorithms, the focus on this study is on increasing the spatial forecasting ability whilst neglecting the forecasting threshold and temporal forecast; both elements will be part of future publications. The methods are all applied individually, by calculating normalized

time-dependent forecasting maps. Each map consists of a spatial grid of values from [0 1], where 0 indicates a very low probability of a future event and 1 a very high probability. The final superposition of the methods is the normalized sum of the applied methods. The relative weighting of the different methods against each other is currently set to be equal, but it has been tested to identify whether a certain method contributes significantly more to a better forecast than another.

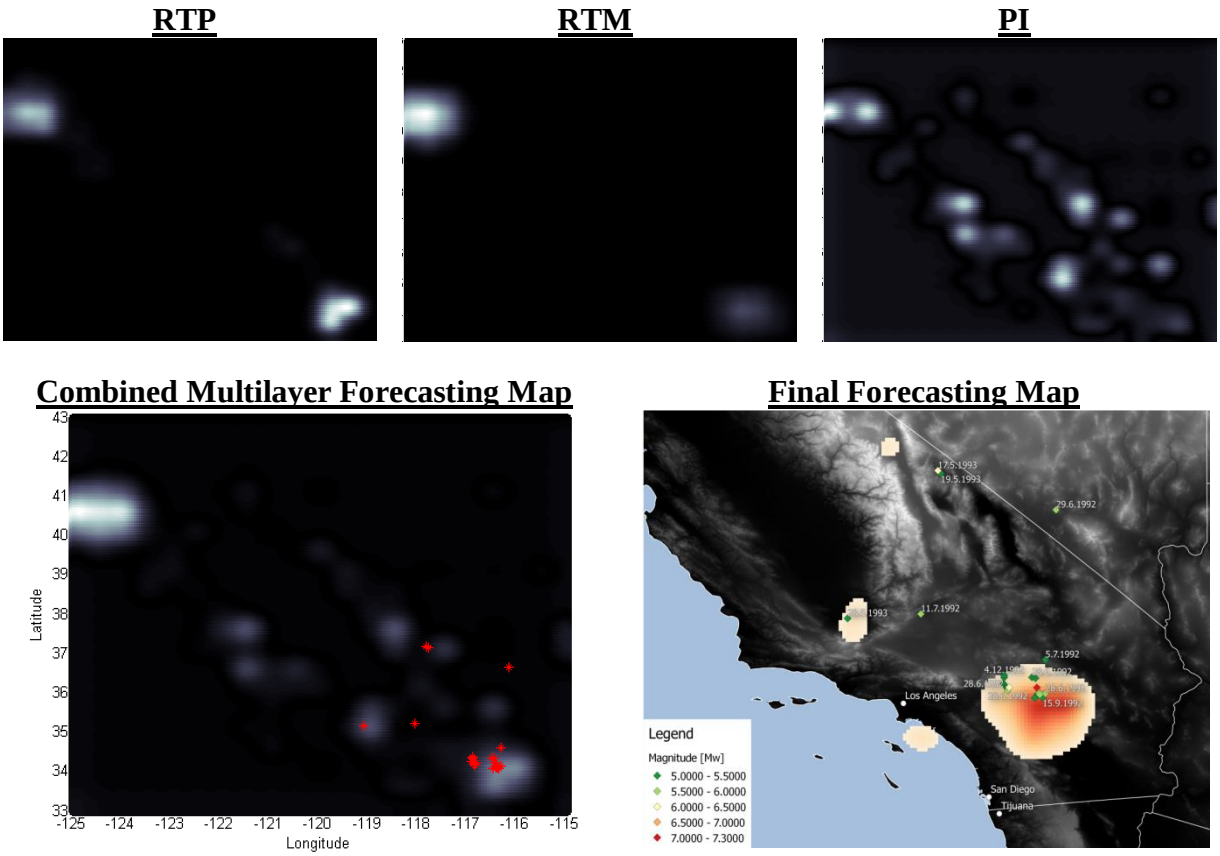

Figure 2: Comparison of the three maps produced for June 21st, 1992, 1 day prior to the Landers earthquake sequence. The three maps on top show the independent forecasting maps, while the map in the bottom shows their superposition. The red dots indicate all locations of earthquakes with $M_w \geq 5$ *within the following 12 months. The strong signal in the north-west is related to the* $M_w \geq 7.2$ *event of April 25th, 1992. In the bottom-right corner is the final forecasting map, a superposition with the time-independent smooth seismicity approximation (zoomed in to longitude [-120° -115°] and latitude [33° 38°])*

Since the forecasting maps are evolving over time, the forecasting ability has been tested with respect to most of the major earthquakes in California; whereby the earthquake data of the ANSS [ANSS] has been used since 1975 with a minimum magnitude of Mw>=3. The target events in terms of the temporal timeframe for testing of all events with a magnitude larger than Mw>= 6. 4 time windows have been used, 6 months, 1 month, 1 week and 1 day prior to the main shock. To test the spatial forecasting ability, all earthquakes with Mw>=5 are examined. Table 1 shows the overview of all the target events. Figure 2 shows the combination of 3 forecasting maps originating from the applied methods to the final multilayer forecasting map which has been tested for its spatial forecasting capabilities. As a final step, the multilayer forecasting map can be combined with an alternated time-independent smooth seismicity map. This smooth seismicity map is based on the same clustered earthquake data as the time-dependent forecast and normalized. The absolute values are currently neglected since there is no established link to calculate time-dependent earthquake probabilities in the multilayer framework. Therefore, only the spatial forecasting elements are tested.

5. Results

In total, 12 seismic events have been identified; some of these events consist of multiple subsequent earthquakes such as the 1992 Landers sequence. Focus of the tests was to identify the spatial forecasting capabilities for multiple combinations of the proposed forecasting methods. As mentioned in Chapter 4, the forecasting ability in time and associated threshold values is not evaluated and will be examined in future publications.

Name	Year	Month	Day	Lat (°)	Long (°)	Mw
Mammoth Lakes	1980	5	25	37,6	-118,8	6,1
Coalinga	1983	5	2	36,2	-120,3	6,4
Morgan Hill	1984	4	24	37,3	-121,7	6,2
n/a	1984	11	23	37,5	-118,6	6,1
North Palm Springs	1986	7	8	34,0	-116,6	6
Chalfant Valley	1986	7	21	37,5	-118,5	6,2
Superstition Hills	1987	11	24	33,1	-115,8	6 & 6,5
Loma Prieta	1989	10	17	37,0	-121,9	6,9
Joshua Tree	1992	4	22	34,0	-116,3	6,1
Landers	1992	6	28	34,2	-116,5	7,3 & 6,5
San Simeon	2003	12	22	35,7	-121,1	6,6
Northern Baja California	2010	4	4	32,1	-115,3	7,2

Table 1: Target earthquakes in California for a period between 1980 and 2010.

						Equal Weight				RTP			
Year	Month	Day	Lat (°)	Long (°)	Mw	6m	1m	1w	1d	6m	1m	1w	1d
1980	5	25	37,6	-118,8	6,1	0,96	0,93	0,77	0,84	0,98	0,93	0,86	0,93
1983	5	2	36,2	-120,3	6,4	0,62	0,52	0,40	0,38	0,54	0,45	0,38	0,35
1984	4	24	37,3	-121,7	6,2	0,43	0,41	0,86	0,83	0,25	0,44	0,87	0,84
1984	11	23	37,5	-118,6	6,1	0,93	0,66	0,47	0,45	0,95	0,44	0,36	0,35
1986	7	8	34,0	-116,6	6	0,61	0,98	0,97	1,00				
1986	7	21	37,5	-118,5	6,2	0,47	0,02	0,11	0,92				
1987	11	24	33,1	-115,8	6 & 6,5	0,00	0,51	0,51	0,52				
1989	10	17	37,0	-121,9	6,9	0,10	0,92	1,00	1,00				
1992	4	22	34,0	-116,3	6,1	0,55	0,64	0,62	0,64				
1992	6	28	34,2	-116,5	7,3 & 6,5	0,78	0,87	0,86	0,81		0,81	0,81	0,76
2003	12	22	35,7	-121,1	6,6	0,69	0,55	0,17	0,19	0,69	0,55	0,17	0,19
2010	4	4	32,1	-115,3	7,2	0,90	0,91	0,77	0,78				

						RTM				PI			
Year	Month	Day	Lat (°)	Long (°)	Mw	6m	1m	1w	1d	6m	1m	1w	1d
1980	5	25	37,6	-118,8	6,1	0,95	0,85	0,59	0,77	0,94	0,91	0,77	0,83
1983	5	2	36,2	-120,3	6,4	0,51	0,37	0,32	0,31	0,66	0,70	0,43	0,41
1984	4	24	37,3	-121,7	6,2	0,30	0,45	0,87	0,85	0,62	0,38	0,85	0,81
1984	11	23	37,5	-118,6	6,1	0,96	0,82	0,78	0,74	0,75	0,67	0,38	0,34
1986	7	8	34,0	-116,6	6	0,53	0,92	0,92	0,98	0,63	1,00	1,00	1,00
1986	7	21	37,5	118,5	6,2	0,37	0,03	0,06	0,91	0,41	0,01	0,15	0,94
1987	11	24	33,1	-115,8	6 & 6,5	0,00	0,43	0,44	0,45	0,00	0,58	0,57	0,57
1989	10	17	37,0	-121,9	6,9	0,02	0,97	1,00	1,00	0,26	0,86	1,00	0,99
1992	4	22	34,0	-116,3	6,1	0,52	0,49	0,61	0,63	0,58	0,74	0,63	0,65
1992	6	28	34,2	-116,5	7,3 & 6,5	0,67	0,85	0,84	0,83	0,90	0,64	0,60	0,78
2003	12	22	35,7	-121,1	6,6	0,73	0,35	0,12	0,13	0,57	0,77	0,23	0,25
2010	4	4	32,1	-115,3	7,2	0,67	0,54	0,66	0,66	1,00	0,96	0,99	0,99

Table 2: Results for spatial forecasting tests, using an area skill score system. 1.0 indicates a perfect forecast, while 0 would be a perfect miss. (6m = 6 months, 1m = 1 month, 1w = 1 week, 1d = 1 day prior to indicated main shock).

a) Coalinga - May 2nd, 1983

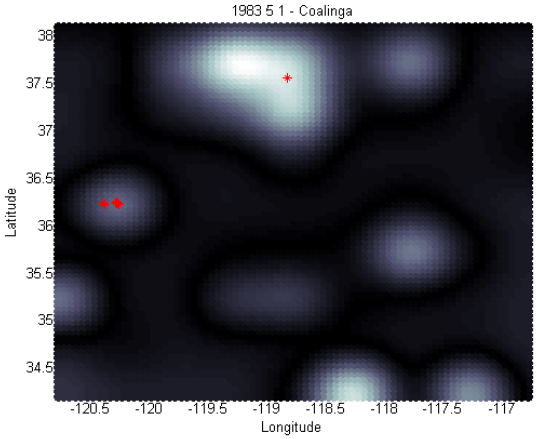

1 day prior to main shock

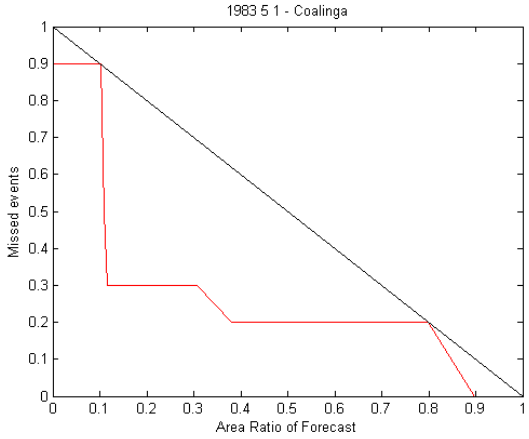

b) Loma Prieta - July 17th, 1989

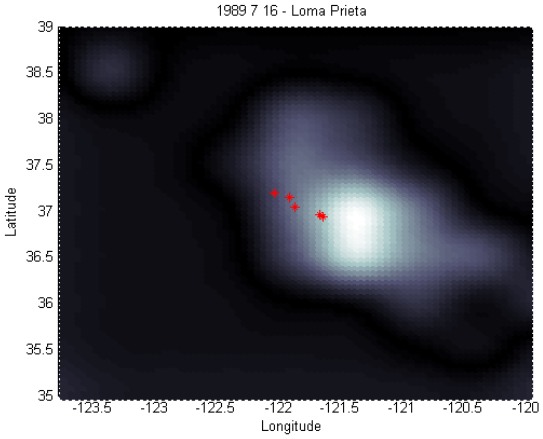

1 day prior to main shock

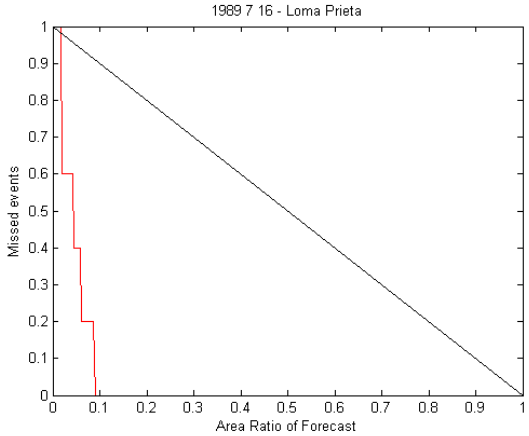

c) Landers - June 22nd, 1992

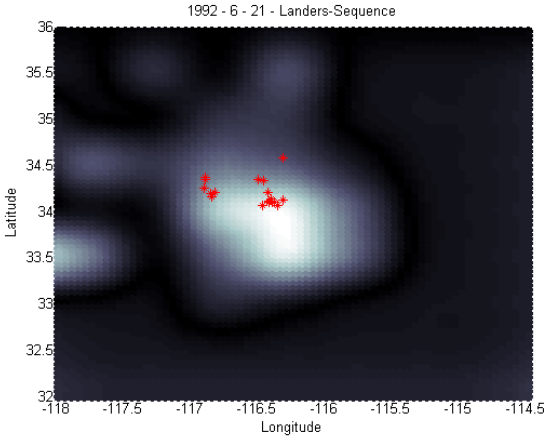

1 day prior to main shock

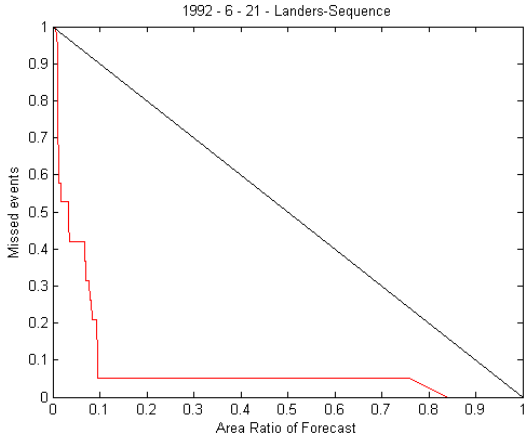

Figure 3: Case studies: Spatial and area skill score results for forecasts a) 1 day prior to the Coalinga earthquake of 1983, b) 1 day prior to the Loma Prieta earthquake of 1989, c) 1 day prior to Landers earthquake sequence of 1992. The red line denotes the forecast, the black one indicates a random forecast

The RTP contribution to the multilayer forecast map depends on the presence of tracked earthquakes chains to the time of the forecast; thus, only 6 of the 12 events had RTP-based elements. For the other 5 events, only the RTM and PI methods have been used for the final map. Testing the quality of the maps is based on the area skill score as described in Zechar [2010] and respective Molchan error diagrams, where it is shown how much space the forecast occupies with respect to the total area to include all target events. A random forecast is shown as a black straight line. The forecast is shown with a red line, as closer the line is to the left hand side and the bottom, indicating a smaller area is occupied for a complete

forecast, as better the forecast is. An overall score is obtained by calculating the integral of the curve for predicted events. Thus, 1.0 indicates a perfect forecast, where the highest forecasting value correlates exactly with the observed earthquakes, while 0.0 shows no correlation between the observed earthquakes and the forecasting map.

Table 2 shows the results for all events for different forecasting periods prior to the main shock. Different combinations of weighting have been examined. In total, 4 different combinations have been tested, one with equal weighting, and three combinations where one method has a doubled weighting with respect to the others. To avoid bias of surrounding seismicity, for each event a spatial window of 400x400 km was investigated centred around the mainshock's epicentre. Figure 3 shows three case results, for Loma Prieta 1989, Landers 1992 and Coalinga 1983. Except for two events, almost all earthquakes occurred in areas where the forecasts indicate a value larger than 0.5. Table 3 gives detailed results for the whole procedure, with the mean forecasting qualities showings that all methods are relatively close to each other in terms of their forecasting capabilities. Each method can show in different events that it is able to outperform the other methods, while in average over all test cases there is no significant difference. The assumption of combining multiple methods leads to an improvement of the general forecasting results.

	Mean Results				
	6m	**1m**	**1w**	**1d**	**Overall**
Equal Weight	0,59	0,66	0,63	0,70	**0,64**
RTP	0,68	0,60	0,58	0,57	**0,61**
RTM	0,52	0,59	0,60	0,69	**0,60**
PI	0,61	0,68	0,63	0,71	**0,66**

Table 3: Average results for the different weighted combinations for different times prior to the main shock and the respective over all mean result.

Except for RTP, all methods tend to increase their predictive quality as they get closer in time to the target earthquake. On average, the PI method tends to result in the best forecasts, but the differences are on average not significantly large. However, as it can be seen from the map produced for the Coalinga earthquakes in Figure 3, there are multiple locations indicated to be prone to earthquakes, which is probably related to the short training period since later results have a stronger indication of a future event.

6. Conclusion

Combining multiple time-dependent forecasting maps to increase their forecasting capabilities can be considered to be promising and, in terms of the first tests, also as successful. For multiple events, retrospective testing has shown that the forecasting accuracy can be significantly increased, and precursory signals which might have been undetected whilst using only one method have been made visible using multiple different pattern recognition approaches.

The current version of the multilayer framework incorporates three different methods, namely the Reverse-Tracing of Precursors roughly following the description of Shebalin et al. [2006], the Pattern Informatics of Kawamura [2014] and the RTM-Method of Huang [2011]. The focus has been on increasing the spatial accuracy of the forecasting approaches, which can be considered successful from the test results presented in Chapter 5. The next step in advancing this tool is subsequent testing in other locations, further parameter adjustments of the implemented methods and the development of time-dependent Gutenberg-Richter parameters to result in daily-based forecasts with distinct magnitude and location-dependent earthquake probabilities.

References

ANSS - Advanced National Seismic System - http://www.ncedc.org/anss/catalog-search.html

Holliday, J.R., Nanjo, K.Z., Tiampo, K.F., Rundle, J.B., Turcotte., D.L., (2005), Earthquake forecasting and its verification, Nonlinear Processes in Geophysics, 12, 967-977, 2005, doi: 1607-7946/npg/2005-12-965

Huang, Q. (2006), Search for reliable precursors: A case study of the seismic quiescence of the 2000 western Tottori prefecture earthquake, J. Geophys. Res., 111, B04301, doi:10.1029/2005JB003982.

Kagan., Y.Y, (1997), Are earthquakes predictable?, Geophys. J. Int., 131, 505-525, 1997

Kawamura, M., Wu, Y.-H., Kudo, T., Chen., C.-c., (2014), A statistical feature of anomalous seismic activity prior to large shallow earthquakes in Japan revealed by the pattern informatics method, Nat. Hazards Earth Syst. Sci., 14, 849-859, 2014, doi: 10.5194/nhess-14-849-2014

Kossobokov, V.G., (1986). The test of algorithm M8. In: Gabrielov, A., Dmitrieva, O.E., Keilis-Borok, V.I., Kossobokov, V.G., Kuznetsov, I.V., Levshina, T.A., Mirzoev, K.M., Molchan, G.M., Negmatullaev, S.Kh, Pisarenko, V.F., Prozoroff, A.G., Rinehart, W., Rotwain, I.M., Shebalin, P.N., Shnirman, M.G., Shreider, S.Yu (eds.), Algorithms of Long-term Earthquakes' Prediction. Centro Regional de Sismologia para America del Sur (CERESIS), Lima, Peru, pp. 42 e 52.

Kossobokov, V.G., (2014), Times of Increased Probabilities for Occurrence of Catastrophic Earthquakes: 25 Years of Hypothesis Testing in Real Time, Earthquake Hazard, Risk and Disasters, Hazards and Disasters Series, Volume one, Volume Editor Max Wyss, Series Editor John F. Shroder, Elsevier, 478-504 , ISBN: 978-0-12-394848-9

Nagao, T., Takeuchi, A., Nakamura, K. (2010), A new algorithm for the detection of seismic quiescence: introduction of the RTM algorithm, a modified RTL algorithm, Earth Planets Space, 63, 315-324, 2011, doi: 10.5047/eps.2010.12.007

Schaefer, A., Daniell, J.E., Bunge, H.-P. (2014), State-of-the-Art Review of Earthquake Forecasting Algorithms, Geological Society of Australia, 2014 Australian Earth Sciences Convention (AESC), Sustainable Australia. Abstract No 03ISC-P01 of the 22nd Australian Geological Convention, Newcastle City Hall and Civic Theatre, Newcastle, New South Wales. July 7 - 10, pp. 289 - 290.

Shebalin, P., Keilis-Borok, V., Grabrielov, A., Zaliapin, I., Turcotte, D., (2006), Short-term earthquake prediction by reverse analysis of lithosphere dynamics, Tectonophysics, 413, 63-75, 2006, doi: 10.1016/j.tecto.2005.10.033

Zechar, J.D. (2010), Evaluating earthquake predictions and earthquake forecasts: a guide for students and new researchers, Community Online Resource for Statistical Seismicity Analysis, doi:10.5078/corssa-77337879. Available at http://www.corssa.org.